

Dynamic Instabilities in Resonant Tunneling Induced by a Magnetic Field

P. Orellana,¹ E. Anda,² and F. Claro³

¹*Departamento de Física, Universidad Católica del Norte, Angamos 0610, Casilla 1280, Antofagasta, Chile*

²*Departamento de Física, Pontificia Universidade Católica do Rio de Janeiro, Caixa Postal 38071, 22452-970 Rio de Janeiro, Brasil*

³*Facultad de Física, Pontificia Universidad Católica de Chile, Vicuña Mackenna 4860, Casilla 306, Santiago 22, Chile*
(Received 30 December 1996)

We show that the addition of a magnetic field parallel to the current induces self-sustained intrinsic current oscillations in an asymmetric double barrier structure. The oscillations are attributed to the nonlinear dynamic coupling of the current to the charge trapped in the well, and the effect of the external field over the local density of states across the system. Our results show that the system bifurcates as the field is increased, and may transit to chaos at large enough fields. [S0031-9007(97)03630-2]

PACS numbers: 73.40.Gk, 72.15.Gd

Since the first observation of resonant tunneling through a semiconductor double barrier structure (DBS) by Chang, Esaki, and Tsu, devices based on this structure have been found to exhibit a variety of interesting physical properties [1]. Besides a peak due to simple resonant transmission, structures arising from phonon [2] and plasmon-assisted [3] resonant tunneling, as well as from Landau level matching [4,5], have been observed. Moreover, an intrinsic dynamical bistability and hysteresis in the negative differential resistance region of the current-voltage characteristic has been reported [4,6,7]. This is a nonlinear effect produced by the Coulomb repulsion experienced by the incoming electrons from the charge buildup in the space between the barriers [6].

Qualitative arguments given by Ricco and Azbel [8] suggest the existence of intrinsic oscillations in a DBS for the one-dimensional case. When the energy of the incoming electrons matches the resonance energy they enter the device and charge the potential well, lifting its bottom, thus driving the system away from resonance. The ensuing current decrease lowers the charge in the well bringing the system back to resonance, and a new cycle in an oscillatory behavior begins. Numerical calculations support this prediction for ballistic electrons provided they are not monoenergetic, and in fact their energy spread is comparable, or wider than the resonance width [9].

In this Letter we report the presence of sustained intrinsic oscillations when the source is a Fermi sea of electrons, as one normally has in DBS devices. The oscillations may be regular or irregular, and are made possible by the presence of a magnetic field applied in the direction of the current. They arise thanks to the drastic change that the field causes on the density of states, and from the magnetic field induced enhancement of the nonlinearity of the system, as described below.

Consider a DBS device. In order to study its time evolution under a bias we adopt a first-neighbors tight-binding model for the Hamiltonian. Inclusion of a magnetic field B in the growth direction, henceforth called the z direction,

is simple if a parabolic energy dispersion parallel to the interfaces is assumed. The field quantizes the motion of the electrons in the xy plane, giving rise to Landau levels with energies $\epsilon_n = (n + 1/2)\hbar\omega_c$, where $n = 0, 1, 2, \dots$ is the Landau index and $\omega_c = eB/m^*c$ is the cyclotron frequency. To a good approximation the longitudinal degrees of freedom are decoupled from the transverse motion and may be treated independently. The probability amplitude $b_j^{n\alpha}$ for an electron in a time dependent state $|\alpha\rangle$ to be at plane j along z and in the Landau level n is determined by the equation of motion

$$i\hbar \frac{db_j^{n\alpha}}{dt} = \left(\epsilon_j + \epsilon_n + U \sum_{m\beta} |b_j^{m\beta}|^2 \right) b_j^{n\alpha} + v(b_{j-1}^{n\alpha} + b_{j+1}^{n\alpha} - 2b_j^{n\alpha}), \quad (1)$$

where v is the hopping matrix element between electrons in nearest neighbor planes, and ϵ_j represents the band contour and external bias. Here the sum over (m, β) covers all occupied electron states of the system, within the various Landau levels m with energies below the Fermi level, incident on the DBS from the emitter side. In writing Eq. (1) we have adopted a Hartree model for the electron-electron interaction, keeping just the intra-atomic terms as measured by the effective coupling constant U . We have neglected inter-Landau level transitions since they are of little importance at not too low magnetic fields [10], and averaged over allowed transitions between degenerate states within a Landau level, taking advantage of the localization induced by the Gaussian factor in the Landau basis. Detailed inclusion of long range effects make numerical calculations more difficult, without introducing a qualitative difference in the physical description of the system. As we will show in what follows, the nonlinear term proportional to U appearing in Eq. (1) is of key importance in the behavior of the system.

The time dependent Eq. (1) is solved using a half-implicit numerical method which is second-order accurate and unitary [11]. Discretizing the time variable, it can be

written in the form

$$\begin{aligned} & \frac{1}{2}[b_{j-1}^{n\alpha}(t + \delta t) + b_{j+1}^{n\alpha}(t + \delta t)] + \left\{ \frac{i}{\delta t v} - 1 - 2v[\epsilon_j + \epsilon_n + V_j^Q(t)] \right\} b_j^{n\alpha}(t + \delta t) \\ & = -\frac{1}{2}[b_{j+1}^{n\alpha}(t) + b_{j+1}^{n\alpha}(t)] + \left\{ \frac{i}{\delta t v} + 1 + 2v[\epsilon_j + \epsilon_n + V_j^Q(t)] \right\} b_j^{n\alpha}(t), \quad (2) \end{aligned}$$

where $V_j^Q(t) = U \sum_{m\beta} |b_j^{m\beta}(t)|^2$ and δt is the time increment. In solving the tridiagonal matrix of Eq. (2), boundary conditions must be specified at the left ($z = -L$) and right ($z = L$) edges of the structure. The approach taken here assumes that in the presence of a bias, the wave function at time t outside the structure is given by [11]

$$b_j^{n\alpha} = I e^{ik_\alpha z_j} + R_{jn} e^{-ik_\alpha z_j}, \quad z_j \leq -L, \quad (3)$$

$$b_j^{n\alpha} = T_{jn} e^{ik'_\alpha z_j}, \quad z_j \geq L. \quad (4)$$

Here k_α and $k'_\alpha = \sqrt{2m^*[\epsilon_\alpha - \epsilon_L]}/\hbar$ are the wave numbers of the incoming and outgoing states, respectively, with $\epsilon_\alpha = \epsilon_n - 4v \sin^2(k_\alpha a/2)$ the energy of the incoming particle. To model the interaction with the particle reservoir outside the structure the incident amplitude I is assumed to be a constant independent of the coordinates. The envelope function of the reflected and transmitted waves, R_{jn} and T_{jn} , are allowed to vary with j , however. Since far from the barriers these quantities are a weak function of the coordinate z_j we restrict ourselves to the linear corrections only. This approximation is appropriate provided the time step δt does not exceed a certain limiting value. For the results presented here, a maximum value of $\delta t = 3 \times 10^{-17}$ s was found sufficient to eliminate spurious reflections at the boundary while maintaining numerical stability up to 20×10^{-12} s.

In our numerical procedure the coefficients obtained for one bias are used as the starting point for the next bias step. Once $b_j^{n\alpha}$ are known, the current at site j is numerically obtained from [11]

$$J_j = \frac{e}{\hbar(\pi l_m)^2} \sum_n \int_0^{k_{nf}} \text{Im}[b_j^{*n\alpha}(b_{j+1}^{n\alpha} - b_j^{n\alpha})] dk_\alpha, \quad (5)$$

where $l_m = (\hbar c/eB)^{1/2}$ is the magnetic length, $k_{nf} = \sqrt{2m^*(\epsilon_f - \epsilon_n)}/\hbar$ with ϵ_f the Fermi energy, and the sum is over magnetic energies $\epsilon_n \leq \epsilon_f$.

We next apply our model to an asymmetric GaAs/AlGaAs double barrier structure, with emitter and collector barrier thicknesses of 1.12 nm (2 sites) and 3.36 nm (6 sites), respectively, and a well thickness of 11.2 nm (20 sites). The second barrier is made wider than the first in order to enhance the trapping of charge in the well. For this geometry the first resonance at zero bias and magnetic field occurs at 30 meV. The conduction band offset is set at 300 meV. The buffer layers are uniformly doped up to 3 nm from either barrier, so as to give a neutralizing free carrier concentration of $2 \times 10^{17} \text{ cm}^{-3}$ at the contacts. In equilibrium and at $B = 0$ T, the Fermi level lies 19.2 meV above the asymptotic conduction band edge, so

that the zero bias resonance lies well above the Fermi sea. The parameter values in Eq. (1) are set at $v = -2.16$ eV and $U = 100$ meV. The latter was chosen phenomenologically so as to fit the experimental I - V characteristic for a GaAs device in the absence of an external magnetic field [4].

For small values of the magnetic field a stationary solution is reached after a short transient. At large enough bias two stationary solutions emerge, however, reached separately by either increasing or decreasing the applied voltage. In the former case the solution sustains a charged well while in the latter the well is uncharged and the current is very small. The effects mentioned have been observed experimentally [5] and are presently well understood [12].

A completely novel feature starts to develop as the magnetic field is increased. At small values of the external bias a stationary solution is rapidly reached. As the bias is increased, however, a critical value arises beyond which no stationary solution exists, and the system begins to oscillate in a self-sustained way. After a range of voltages over which the oscillations persist a stationary solution is reached again. This is illustrated in Fig. 1 where the I - V characteristic for an applied field of 13 T is exhibited. The lobe in the figure shows the current maxima and minima in the unstable region, its size and location depending sensitively on the magnetic field. For the case of Fig. 1 its onset is at a rather low bias and reaches into the bistable region, while at lower magnetic fields the lobe is entirely

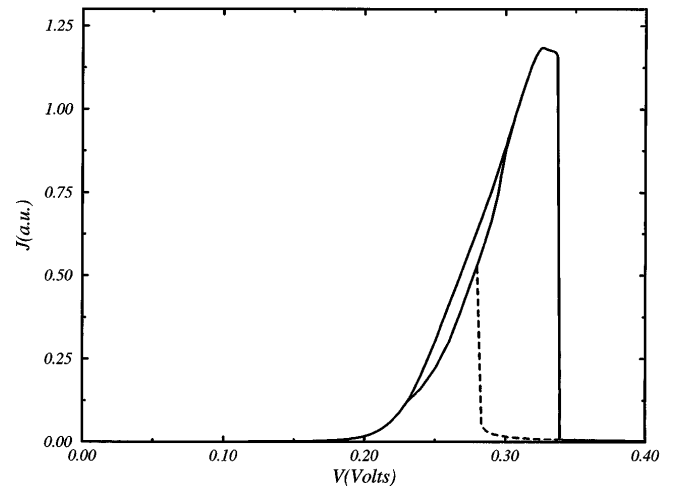


FIG. 1. I - V characteristic of the asymmetric DBS at $B = 13$ T. The lobe edges mark the oscillation extremes when an unstable solution is present. The dashed line represents the lower arm of the bistable regime, reached when the bias is being decreased.

contained in the low bias range, and lies outside the region of bistability. In fact, our results show that the well known bistability and the magnetic field induced instability are entirely separate phenomena.

In Fig. 2 we show the current at the center of the well for three different values of the magnetic field and a fixed bias $V = 0.27$ V. For $B = 9$ T, the system is seen to reach a stationary state after a transient lasting about 5 ps [Fig. 2(a)]. For $B = 13$ T, however, the transient is followed by an oscillation that is never damped out [Fig. 2(b)]. Although not perfectly periodic, the oscillation has two strong Fourier components at frequencies

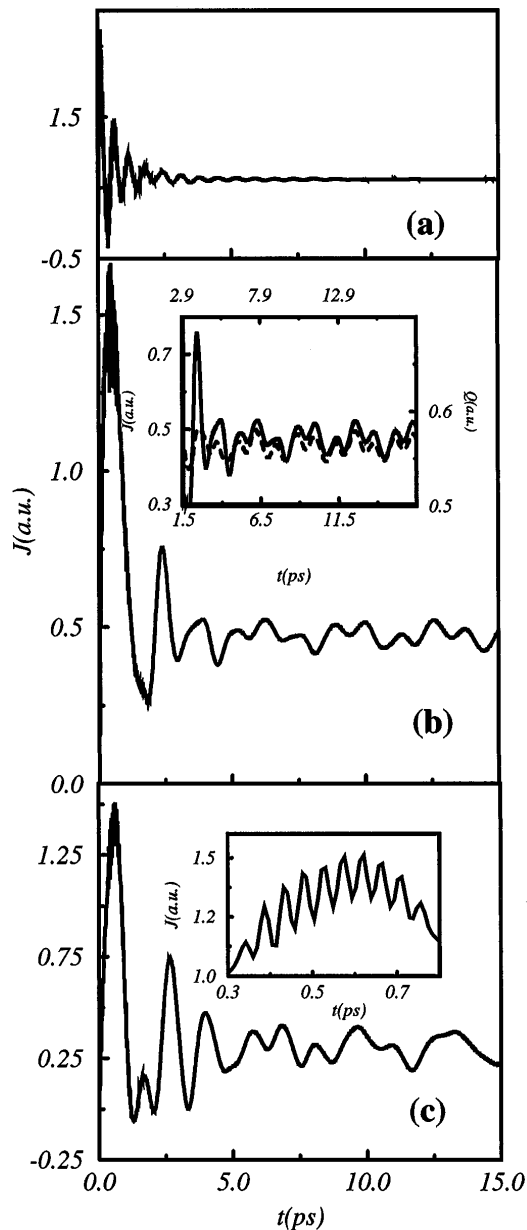


FIG. 2. Current as a function of time at the center of the well for $V = 0.27$ V and an applied magnetic field of (a) 9 T, (b) 13 T, and (c) 17 T. The inset in (b) shows the charge and current shifted one relative to the other by 1.4 ps. The inset in (c) exhibits a detail of the high frequency transient oscillations.

$\nu \sim 0.3$ and 0.8 THz. The reason why the presence of two frequencies is predominant remains unclear. As shown in Fig. 2(c) for $B = 17$ T, at still higher magnetic fields the oscillation becomes irregular. A power spectrum of this latter signal shows that the narrow peaks observed below 1 THz are replaced by a broad low frequency structure suggesting that a chaotic regime has been reached. Note that the initial condition from which all three curves were obtained is the stable solution at 0.2 V. When reaching a bias of 0.27 V from a closer voltage the transient oscillations are less pronounced, yet their relaxation time is of the same order as in the more extreme voltage jump exhibited in the figure. Although the amplitude of the sustained oscillations depends somewhat on the initial conditions, their frequency and structure does not.

Figure 3 shows the regions where the various structures we have described appear in the two parameter space B, V . The thick lines delimit the range in which two stable solutions may exist for the same applied potential. The dotted regions mark areas where self-sustained oscillatory solutions appear. Regions with highly irregular oscillations suggesting a chaotic behavior appear filled with a brick design. We note that while we include in our simulations up to several hundred thousands time steps, the number of oscillations covered before numerical instabilities arise is not enough to obtain a fully detailed power spectrum at all values of parameters. The search of stationary solutions using a standard self-consistent iterative loop, however, did show unambiguously a transition to chaos through successive bifurcations within the region where no stationary solutions exist. Although the iteration number in this case is not a true time variable, the parameter values at which nonstationary solutions exist and the nature of the latter coincide with those obtained in the true-time-dependent analysis. We used this fact in sketching Fig. 3.

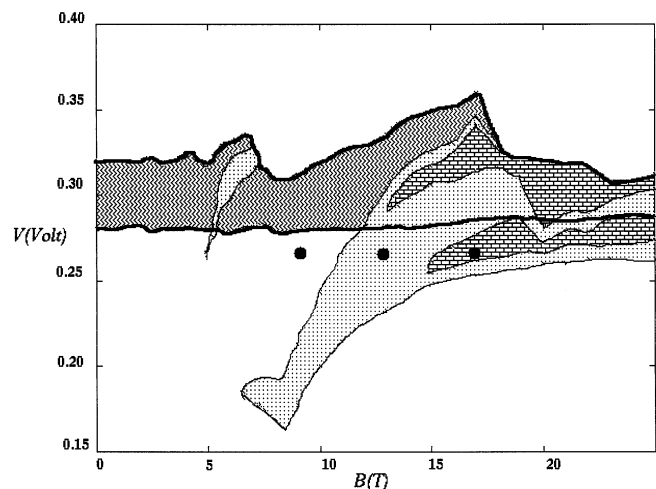


FIG. 3. Phase diagram in the B, V parameter space. The thick lines delimit the region where bistability occurs. Dotted areas correspond to oscillatory behavior, while the brick design marks the regions where highly irregular solutions are present. The filled circles mark the values used in Fig. 2.

We interpret our findings in the following way. In general, current flows through the system as long as a tunneling resonance lies within the emitter Fermi sea. The resonance acts effectively as an energy filter for the transmitted electrons. We assume that at very low bias it lies above the Fermi energy so that no current flows. As the bias increases the resonance drops, reaching eventually the Fermi energy, thus opening a channel for electrons to tunnel through the double barrier. A current is thus established. What happens next depends sensitively on the presence or absence of a magnetic field. In the absence of the electron-electron interaction the current, roughly speaking, grows linearly with the bias if $B = 0$. This behavior is due to the gradual increase in tunneling states that satisfy the conservation laws as the voltage is raised. At a critical bias the falling resonance reaches the bottom of the conduction band, after which the current drops abruptly. This overall behavior gives the I - V curve its characteristic triangular shape. For finite B , however, also in the absence of electron-electron interaction, owing to the new density of states each time a Landau level enters the Fermi sea the current rises abruptly, remaining essentially constant until the next level comes in. The I - V curve acquires then a staircase shape, with a step rise made smooth by the resonance line shape. When the resonance reaches the bottom of the first Landau level in the emitter, the current falls abruptly, as in the $B = 0$ case.

We next take into account the electron-electron interaction. As the resonance enters the Fermi sea, current begins to flow and charge is trapped in the potential well, raising its bottom and pushing the resonance towards higher energies. The current drops, some of the accumulated charge leaks out allowing the current to flow more easily once again, and a new cycle begins. When $B = 0$ this process occurs at very low current, and as we have verified numerically, the ensuing oscillations are damped out in all cases. At finite field, however, as the resonance enters the Fermi sea, the abrupt rise of the current to a large value triggers oscillations that may be sustained by the feedback mechanism if the field is large enough.

The transition from damped to sustained oscillations may be appreciated in Fig. 2. As the magnetic field is raised, the degeneracy of the resonance increases thus allowing more charge to be trapped between the barriers. The nonlinear coupling in Eq. (1) thus grows with the field, making the latter an effective tunable parameter for the amount of nonlinearity in the system. Note also that while the dynamic bistability characteristic of DBS is related to the drop of the resonance below the bottom of the Fermi sea, the effect we are discussing arises as the resonance enters the Fermi sea, in support of our numerical finding that they are entirely independent effects.

According to the picture drawn above the charge in the well lags the current, as exhibited in the inset of Fig. 2(b). Here the charge at the center of the well (dashed line) is plotted together with the current at the same point (full line), the former displaced a time $\tau \sim 1.4$ ps to the left

with respect to the latter. The relaxation time τ and the period of the oscillations are determined by the tunneling time for the electrons to leak out through the barriers and may be adjusted by modifying the barrier thicknesses. The oscillatory current is always nonuniform across the device, with prominent oscillations in the well and the emitter side, while the collector current exhibits a weaker structure. This is due to the large width of the collector barrier relative to that in the emitter side, a necessary feature of design to have enough charge accumulation in the well, and thereby, a strong electron-electron interaction. In fact, nonlinear effects disappear in our sample if the width of the collector barrier is reduced from six to just three sites, in agreement with experimental observations [13]. The very high frequency oscillations seen early in the process and shown in the inset of Fig. 2(c) are quickly damped out and do not contribute to the long term behavior of the system. We attribute them to a transient pulse going back and forth in the space between the barriers before it loses coherence and decays. Its period corresponds to electrons at the Fermi velocity being successively reflected by the barriers in the well region.

There is a wide region of accessible values of bias and magnetic field where oscillatory currents are either present or absent. This opens up the interesting and unique possibility of studying experimentally the transition from stationary to oscillatory behavior and possibly chaos, as the magnetic field is increased in an asymmetric DBS device under bias. When oscillating, the system could act as an electromagnetic generator in the THz region. Research incorporating the interaction between the current and the radiation field is currently under progress.

Work supported by FONDECYT Grants No. 1950190 and No. 1960417, Fundación Antorchas/Vitae/Andes Grant No. B-11487/4B005, CNPq, and FINEP.

-
- [1] L.L. Chang, L. Esaki, and R. Tsu, *Appl. Phys. Lett.* **24**, 593 (1974).
 - [2] V.J. Goldman, D.C. Tsui, and J.E. Cunningham, *Phys. Rev. B* **36**, 7635 (1987).
 - [3] C. Zhang, M.L.F. Lerch, A.D. Martin, P.E. Simmonds, and L. Eaves, *Phys. Rev. Lett.* **72**, 3397 (1994).
 - [4] A. Zaslavsky, V.J. Goldman, D.C. Tsui, and J.E. Cunningham, *Appl. Phys. Lett.* **53**, 1408 (1988).
 - [5] A. Zaslavsky, D.C. Tsui, M. Santos, and M. Shayegan, *Phys. Rev. B* **40**, 9829 (1989).
 - [6] V.J. Goldman, D.C. Tsui, and J.E. Cunningham, *Phys. Rev. Lett.* **58**, 1256 (1987).
 - [7] T.C.L.G. Sollner, *Phys. Rev. Lett.* **59**, 1622 (1987).
 - [8] B. Ricco and M. Ya. Azbel, *Phys. Rev. B* **29**, 1970 (1984).
 - [9] G. Jona-Lasinio, C. Presilla, and F. Capasso, *Phys. Rev. Lett.* **68**, 2269 (1992).
 - [10] D. Yoshioka and P. A. Lee, *Phys. Rev. B* **27**, 4986 (1983).
 - [11] R. Mains and G. Haddad, *J. Appl. Phys.* **64**, 3564 (1988).
 - [12] P. Orellana, F. Claro, E. Anda, and S. Makler, *Phys. Rev. B* **53**, 12967 (1996).
 - [13] L. Eaves, M.L. Leadbeater, and C.R.H. White, *Physica (Amsterdam)* **175B**, 263 (1991).